Vol. 62: 79–97, 2015
doi: 10.3354/cr01261

CLIMATE RESEARCH
Clim Res

Published online January 14

Projecting streamflow in the Tangwang River basin (China) using a rainfall generator and two hydrological models

Wenbin Liu[1,*], Aijing Zhang[2], Lei Wang[1], Guobin Fu[3], Deliang Chen[4], Changming Liu[5], Tijiu Cai[6]

[1]Key Laboratory of Tibetan Environment Changes and Land Surface Processes, Institute of Tibetan Plateau Research, Chinese Academy of Sciences, Beijing 100101, PR China

[2]Center for Water Research, College of Engineering, Peking University, Beijing 100871, PR China

[3]CSIRO Land and Water, Private Bag 5, Wembley, Western Australia 6913, Australia

[4]Department of Earth Sciences, University of Gothenburg, Gothenburg 40530, Sweden

[5]Key Laboratory of Water Cycle and Related Land Surface Processes, Institute of Geographic Sciences and Natural Resources Research, Chinese Academy of Sciences, Beijing 100029, PR China

[6]School of Forestry, Northeast Forestry University, Harbin 150040, PR China

ABSTRACT: To estimate the impacts of future climate change on streamflow in the Tangwang River basin (TRB) in northeastern China, 2 hydrological models, the Soil and Water Assessment Tool and the Hydro-Informatic Modeling System, were used. These models are driven by future (2021–2050) local rainfall and temperature scenarios downscaled from global climate model (GCM) simulations from the fifth phase of the Coupled Model Intercomparison Project under 2 emission scenarios (Representative Concentration Pathway [RCP] 4.5 and RCP8.5). The downscaling of rainfall is done with the help of a multisite stochastic rainfall generator (MSRG), which extends the 'Richardson type' rainfall generator to a multisite approach using a modified series-independent and spatial-correlated random numbers method by linking its 4 parameters to large-scale circulations using least-squares regressions. An independent validation of the MSRG shows that it successfully preserves the major daily rainfall characteristics for wet and dry seasons. Relative to the reference period (1971–2000), the annual and wet season (April to October) streamflow during the future period (2021–2050) would decrease overall, which indicates that water resources and the potential flood risk would decline in the TRB. The slightly increased dry season (November to March) streamflow would, to some extent, contribute to the 'spring drought' over this region. Although rainfall is projected to remain unchanged in the wet season and the whole year, the increased total evapotranspiration due to the increase in temperature would lead to a decline in total streamflow for this basin. The projected streamflow changes from multiple GCMs in this paper could provide a glimpse into a very plausible future for the water resource management community, and would hence provide valuable references for the sustainable management of water and forest ecosystems under a changing climate.

KEY WORDS: Multisite stochastic rainfall generator · Statistical downscaling · CMIP5 · Soil and Water Assessment Tool · SWAT · Hydro-Informatic Modeling System · HIMS · Climate change · Tangwang River

1. INTRODUCTION

Incorporating the influences of global climate change and variability into regional water resources planning and management is increasingly necessary to more accurately predict future supplies (Bates et al. 2008, Piao et al. 2010, Fu et al. 2013, Wang et al. 2013). This is particularly crucial for mountain basins, which are key sources of streamflow, and provide significant water yields to downstream users (Kienzle et al. 2012).

*Corresponding author: liuwb@itpcas.ac.cn

The Tangwang River rises from the Xiaoxing'an Mountains in northeastern China and flows into the Songhua River, the basin of which has approximately 85% of its total area under forest cover. The climate in the Tangwang River basin (TRB) has become warmer and drier during the period 1964–2006, contributing to an 86% decrease in total streamflow (W. B. Liu et al. 2013a). The timing and magnitude of snowmelt runoff in this basin has changed significantly because of the temperature increase (W. B. Liu et al. 2013a). These findings are useful for understanding past climate variability and its corresponding impacts, but they are not sufficient to project future changes. This study stemmed from the need to project the future climate and streamflow of the TRB, which is important for addressing climate adaptation issues such as water supply and water use, as well as forest ecosystems management in downstream areas.

Climate models are the primary tools available to simulate future climate impacts under different emission scenarios (Guo et al. 2002, Immerzeel et al. 2010, Chen et al. 2012, Dawadi & Ahmad 2012). However, there is a general consensus among the scientific community that global climate model (GCM)-simulated climate (especially for daily rainfall) cannot be directly used as input to hydrological models, which often operate on spatial scales smaller than those of GCMs (Wilby et al. 2002, Fowler et al. 2007). Statistical downscaling is thus often used to bridge the scale gap in linking GCMs with hydrological models, because it does not require significant computing resources and can more directly incorporate observations into methods compared with dynamic downscaling (Fowler et al. 2007, Maraun et al. 2010). During the past 2 decades, many statistical downscaling models were developed and used for rainfall projections (Wilks 1998, Chandler & Wheater 2002, Fan et al. 2005, Hanssen-Bauer et al. 2005, Wetterhall et al. 2006, Benestad et al. 2008, Liao et al. 2011, W. B. Liu et al. 2013c, Sachindra et al. 2013). Among them, stochastic weather generators (WGs) in various forms have been widely developed for downscaling daily rainfall from GCMs. However, most of the WGs work only for a single site. The observed spatial structure and correlation among multiple stations, which is critical for hydrological modeling, cannot be reasonably simulated (Qian et al. 2002). Although much effort has focused on the development of multisite models (Chandler & Wheater 2002, Charles et al. 2004, Hewitson & Crane 2006, Mehrotra & Sharma 2007, Zheng & Katz 2008, Frost et al. 2011), the spatial models used in most multisite models today are still not sufficient for accessibility. For example, some models are not easily used in relatively large regions because of their inherent model complexities and significant time requirements (Wilks 1998).

A probabilistic downscaling framework was proposed by Schoof et al. (2010), based on the well-known 2-part stochastic rainfall model (Wilks 1998, Mehrotra et al. 2006, Mhanna & Bauwens 2012). It provides a relatively simple and accessible stochastic method for downscaling daily rainfall at the seasonal scale by linking the model parameters (for example, the P_{01} and P_{11} transition probabilities in the rainfall occurrence model) at each station to large-scale atmospheric circulations using ordinary least-squares regressions. However, this approach has 2 major limitations. The first limitation is that the first-order Markov model and gamma distribution used for rainfall occurrence and amount may not always be suitable for other regions. For example, some studies (Wilks 1999, Harrison & Waylen 2000, Wan et al. 2005, Lennartsson et al. 2008) pointed out the shortcomings of the first-order Markov model, and recommended the use of zero- or higher-order Markov chains in some regions; another study indicated that the gamma distribution may sometimes not be the best choice either (Li et al. 2012). The second limitation is that the model does not consider the spatial dependency among multiple sites, which is the biggest challenge in large-scale rainfall modeling (Yang et al. 2005, Zheng & Katz 2008).

Consequently, this study has 2 objectives: (1) a multisite stochastic rainfall generator (MSRG) is proposed by combining the works of Schoof et al. (2010) and Mhanna & Bauwens (2012) to investigate rainfall multisite correlations, which are critical for hydrological modeling; and (2) the impacts of future climate on streamflow in a typical forest basin (TRB) are projected using 2 hydrological models, the Soil and Water Assessment Tool (SWAT) and the Hydro-Informatic Modeling System (HIMS), which are driven by future (2021–2050) local rainfall and temperature scenarios downscaled from GCM simulations from the fifth phase of the Coupled Model Intercomparison Project (CMIP5) under 2 emission scenarios (Representative Concentration Pathway [RCP] 4.5 and RCP8.5).

2. MATERIALS AND METHODS

2.1. Study region

The TRB (Fig. 1) is a typical forest basin in northeastern China and has 4 boreal forest types: temper-

ate coniferous forest, boreal coniferous forest, deciduous and mixed forest (W. B. Liu et al. 2013a). The entire basin ranges in elevation from 78 to 1150 m and covers approximately 21 245 km^2 at latitude 46° 41′ to 48° 45′ N and longitude 128° 06′ to 129° 55′ E. The multiyear averaged temperature and precipitation in the TRB are approximately −1.1°C and 672.9 mm, respectively, during the period 1964–2006. Streamflow is principally generated from direct precipitation, which makes up almost 70% of annual total surface discharge.

2.2. Datasets

Three types of dataset were used in this study: (1) observed historical daily maximum temperature, minimum temperature, solar radiation, humidity, wind speed, daily rainfall and streamflow records for hydrological model calibration and validation (Fig. 1); (2) large-scale reanalysis datasets, used with historical daily rainfall for calibration and validation of the MSRG; and (3) GCM outputs, used as predictors to produce downscaled maximum temperature, minimum temperature and rainfall projections (1971–2000 and 2021–2050).

Observed daily rainfall datasets and streamflow records were acquired from the Yichun Hydrological Bureau; other meteorological datasets were obtained from the China Meteorological Data Sharing Service System (http://cdc.cma.gov.cn). A threshold of 0.1 mm was uniformly used for the rainfall series to determine whether a day is classified as wet or dry in this study. In addition, land use maps (1:100 000) from the 1980s, a soil type map (1:500 000) and soil properties (e.g. soil thickness and soil texture) were prepared for the SWAT model; land use maps were obtained from the Data Sharing Infrastructure of Earth System Science (www.geodata.cn) and soil maps and soil data were obtained from the Chinese Soil Database at the Institute of Soil Science.

To investigate the relationships between daily rainfall and large-scale predictors, we employed a suite of variables, including sea level pressure, temperature, wind speed and specific humidity at the surface and numerous pressure levels (500, 700 and 850 hPa), on a 2.5° × 2.5° grid extracted from the Reanalysis Ddataset 1 of the National Centers for Environmental Prediction/National Center for Atmospheric Research (NCEP/NCAR, www.esrl.noaa.gov/psd/data/gridded/data.ncep.reanalysis.html) (Kalnay et al. 1996). The same predictors were also derived from the monthly output of 15 GCMs (Table 1) under 2 emission scenarios (RCP4.5 and RCP8.5) from the CMIP5 (http://cmip-pcmdi.llnl.gov/cmip5/) archive (Taylor et al. 2012). The GCM predictors with different spatial resolutions were linearly interpolated to a standard 2.5° × 2.5° grid corresponding to the NCEP/NCAR datasets. All predictors used for rainfall downscaling (either from GCMs or the reanalysis dataset) were previously standardized by subtracting the multiyear mean and dividing by the standard deviation for the calibration period (1981–2000). Additionally, maximum and minimum temperatures from the GCMs were also used to calculate transfer factors for temperature downscaling using an empirical downscaling method (described in Section 2.3.3 'Empirical downscaling for minimum and maximum temperature').

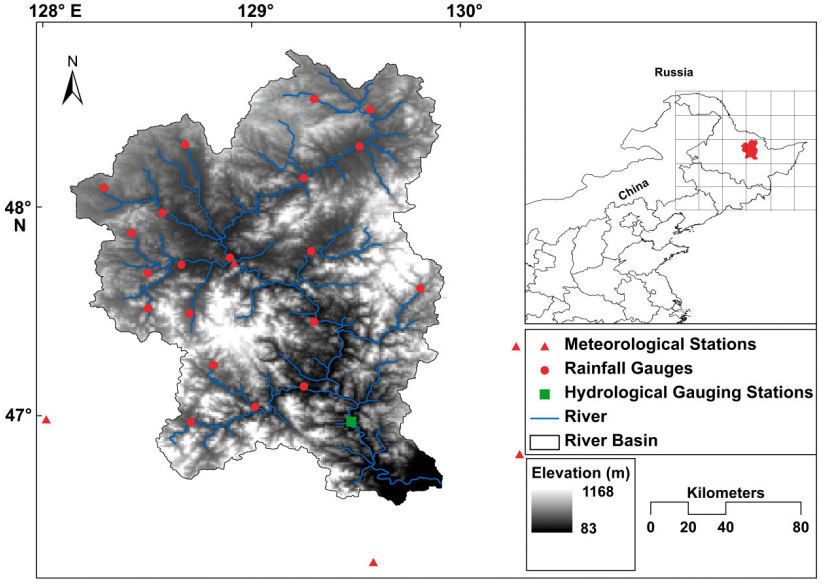

Fig. 1. Tangwang River basin showing locations of the streamflow gauges, meteorological-rainfall stations and grid domain for predictor selection in this study

2.3. Methods

2.3.1. MSRG

Two-part single-site stochastic rainfall generator (SSRG). The 'Richardson type' rainfall generator, perhaps the best-known approach for stochastically simulating the daily rainfall series (Richardson 1981), models the wet and dry day occurrence by a Markov chain,

Table 1. Descriptions of the global climate models from the fifth phase of the Coupled Model Intercomparison Project applied in this study

Model	Institute/country	Atmosphere resolution (° latitude × ° longitude)
ACCESS1.0	CSIRO-BOM/Australia	1.3000 × 1.9000
CSIRO-Mk3.6.0	CSIRO/Australia	1.8750 × 1.8653
CanESM2	CCCMA/Canada	2.8125 × 2.7906
BCC-CSM1.1	BCC/China	2.8125 × 2.7906
CNRM-CM5	CNRM/France	1.4063 × 1.4008
IPSL-CM5B-LR	IPSL/France	1.8750 × 3.7500
MPI-ESM-LR	MPI-M/Germany	1.8750 × 1.8653
CMCC-CMS	CMCC/Italy	3.7500 × 3.7500
MIROC-ESM	MIROC/Japan	2.8125 × 2.7906
MRI-CGCM3	MRI/Japan	1.1250 × 1.1215
NorESM1-M	NCC/Norway	2.8100 × 2.8100
INM-CM4	INM/Russia	2.0000 × 1.5000
HadGEN2-AO	MOHC/UK	1.3000 × 1.9000
GFDL-CM3	NOAA/United States	2.5000 × 2.0000
GISS-E2_H	NASA GISS/United States	2.0000 × 2.5000

and then models the rainfall amount falling on wet days through an appropriate probability density function. Based on this idea, the applicability of 3 Markov chain models (first-, second- and third-order) and three 2-parameter probability distributions (gamma, Weibull and lognormal) were first evaluated for modeling the rainfall occurrence and amount series in this mountain basin by comparing their performance in modeling wet and dry day numbers, mean and maximum wet and dry spell length, as well as daily rainfall distribution (Figs. 2 & 3). The first-order Markov chain model and Weibull distribution were determined to be more suitable to construct the SSRG in this study.

The first-order Markov model assumes that rainfall probability on a certain day is only determined by the wet and dry status of the previous day and is fully defined by 2 transition probabilities: (1) the conditional probability of a wet day after a dry day (P_{01}) and (2) the conditional probability of a wet day after a wet day (P_{11}). The mathematical formulation can be expressed as (Zheng & Katz 2008):

$$P_{j,i} = \Pr(J_{t+1} = i \mid J_t = j) \qquad i, j = 0,1 \quad (1)$$

Here, Pr represents probability, $P_{j,i}$ ($0 < P_{j,i} < 1$) are the transition probabilities and the maximum likelihood estimates, which could be calculated by maximum likelihood estimation as follows:

$$\hat{P}_{01}(k) = \frac{n_{01}(k)}{n_{01}(k) + n_{00}(k)} \quad (2)$$

$$\hat{P}_{11}(k) = \frac{n_{11}(k)}{n_{11}(k) + n_{10}(k)} \quad (3)$$

where for the station k, n_{01}/n_{11} represents the historical counts of wet days following dry and wet days, while n_{00}/n_{10} expresses the historical counts of dry days following dry and wet days. The daily series of rainfall occurrence could then be generated by comparing the appropriate transition probabilities (P_{01} or P_{11}) to a uniform [0,1] random number. If the random number is less than the transition probability, a wet day occurs; otherwise, a dry day occurs.

The probability density function for the Weibull distribution can be given as (Wilks 1989):

$$f(x;\alpha,\beta) = (\beta/\alpha)(x/\alpha)^{\beta-1}\exp[-(x/\alpha)^{\beta}] \qquad (\alpha,\beta,x>0) \quad (4)$$

where the scale parameter α controls the spread of the distribution, and the shape parameter β deter-

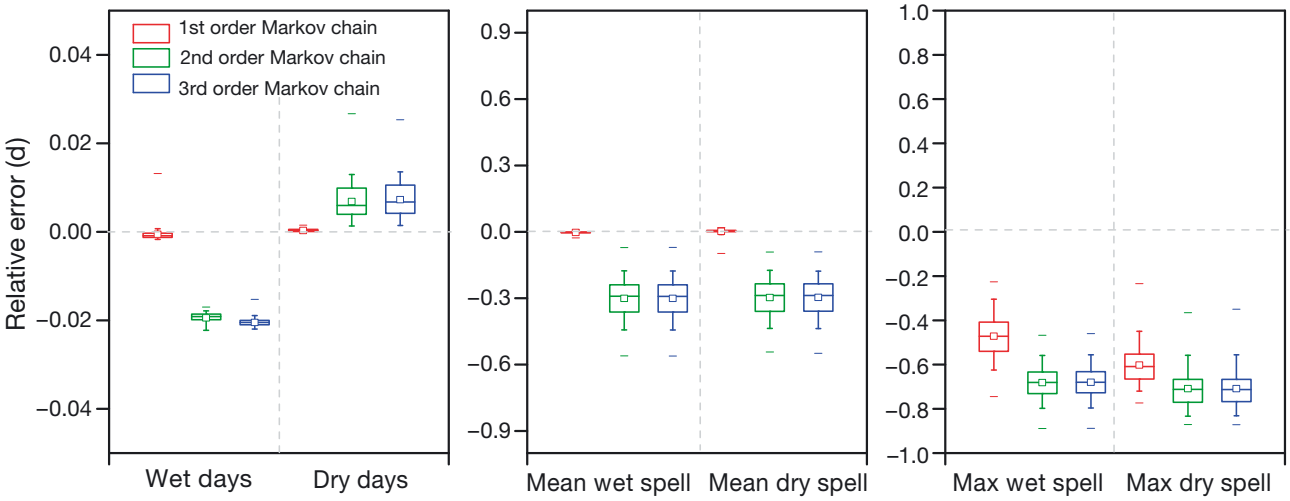

Fig. 2. Comparison of 3 Markov chains (first-, second- and third-order) for modeling (a) annual wet and dry days, (b) mean and (c) maximum wet and dry spell length in the Tangwang River basin. Boxplots — upper and lower dashes: outliers; whiskers: minimum and maximum values; boxes: 1st and 3rd quartiles; central line: median; small square: mean

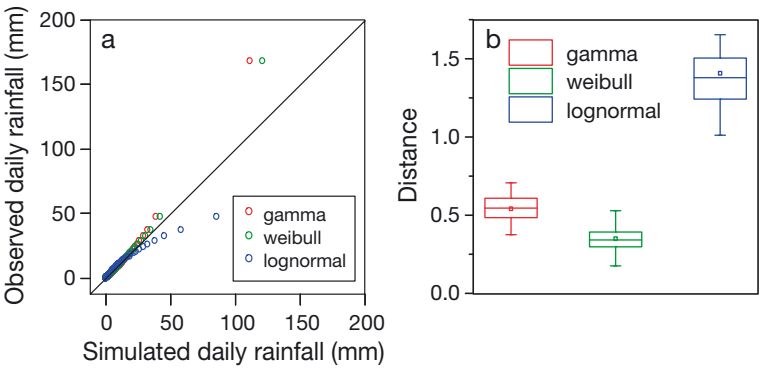

Fig. 3. Comparison of performance of three 2-parameter distributions (gamma, Weibull and lognormal) for modeling daily rainfall amount in the Tangwang River basin. (a) Q-Q plot for different probability distributions. The boxplots in (b) show the minimum, quartile (Q) 1, median, mean (square), Q3 and maximum values of simulated average distances for three 2-parameter distribution. Distance (y-axis): mean distance from the scattered points to the 1:1 reference line in the Q-Q plot

mines the form of the distribution. Once the parameters of Weibull distribution are estimated, the rainfall amount falling on wet days could be stochastically sampled from the probability density function by conditioning on another random number.

Multisite extension of SSRG. As mentioned above, 2 sets of random numbers were adopted in the SSRG for controlling the stochastic generation of the daily rainfall occurrence and amount series for each individual station. The independently reproduced rainfall products could not incorporate the spatial correlation information among all rainfall stations, which is critical for hydrological modeling. Therefore, the basic idea for extending the SSRG to a multiple sites is to replace the single random numbers with series-independent and spatial-correlated random numbers (SSRNs) in the model structure to generate multisite correlated random numbers, and then control generation of the daily rainfall occurrence and amount series for all stations simultaneously. The SSRN (ω_t) was widely used for modeling spatial dependencies in multisite stochastic rainfall models (Wilks 1998, Mehrotra & Sharma 2007). It could be generated from a multivariable Gaussian process with mean zero and variance-covariance matrix Ω:

$$\omega_t = B\varepsilon_t \quad (5)$$

where ε_t is an independent normal vector, and B is the coefficient matrix, which could be calculated as:

$$BB^T = \Omega \quad (6)$$

The variance-covariance matrix Ω could be obtained by rescaling the desired correlations of random numbers by pre- and post-multiplying by a diagonal matrix that contains the standard deviations of each random number series. Once the Ω is calculated, the elements in B could be obtained using Cholesky's decomposition (less than 5 samples) or singular value decomposition (5 or more samples).

Therefore, the most essential procedure for SSRN generation is to estimate the desired correlations in the multisite random numbers, which correspond to the correlations between the observed rainfall occurrence and amount series. The widely used method for this purpose is to fit the empirically derived curves (EDCs) between the random variates correlation [$\omega(k,l)$] and the generated occurrences correlation [$\xi(k,l)$] for each station pair and every monthly period. Then, the desired correlation of random numbers could be estimated by finding the value that corresponds to $\xi^0(k,l)$, the observed value of $\xi(k,l)$, from the empirically derived curve (Wilks 1998). During the past 2 decades, although many methods such as the nonlinear root-finding algorithm (Srikanthan & Pegram 2006), trial and error procedure (Mehrotra et al. 2006), hidden covariance model (Srikanthan & Pegram 2009) and maximum likelihood method (Thompson et al. 2007) were developed for estimating the needed correlation in a more convenient way, they were still significantly time consuming because of the numerous iterative computations, and may sometimes result in the non-positive definiteness problem in Ω. To overcome these limitations, Mhanna & Bauwens (2012) proposed a modified SSRN method for simplifying the calculation of needed correlations between the random numbers. It replaces the widely used EDC algorithm with a gamma coefficient and a rank correlation method when calculating the desired correlations of multisite random numbers in rainfall occurrence and amount models.

More details about how the EDC algorithm can be simplified as well as how the gamma coefficient and rank correlation method could be incorporated into the stochastic models are found in Mhanna & Bauwens (2012). In this paper, we simply introduce the 2 methods. The gamma coefficient method is an appropriate measure that relies only on the joint probabilities of rainfall occurrence between 2 stations (the EDC algorithm considered both the joint probabilities and marginal probabilities, but the $\omega(k,l)$ was shown to have no significant influences on the marginal probabilities), which assumes that the needed

correlations are equal to the gamma correlation between the observed multisite rainfall occurrence series. The gamma correlation could be expressed as:

$$\gamma(k,l) = \frac{\phi(k,l)-1}{\phi(k,l)+1} \quad (7)$$

$$\phi(k,l) = \frac{\pi_{00}(k,l)\pi_{11}(k,l)}{\pi_{10}(k,l)\pi_{01}(k,l)} \quad (8)$$

where $\varphi(k,l)$ represents the odds ratio, while $\pi_{00}(k,l)$ and $\pi_{11}(k,l)$ are the joint probabilities that station pairs are both wet and dry. Additionally, the nonlinear transformation from SSRN-reproduced correlated normal variates to uniform marginal distribution will influence the dependence between the random normal variables (Eqs. 6 & 7). To overcome this problem, Spearman rank correlation $\rho(k,l)$ and its corresponding binomial correlation $\zeta(k,l)$, which preserve the SSRN dependences under any monotonic transformation, were used to calculate the desired correlations of random numbers related to the observed rainfall amount series. The corresponding binomial correlation $\zeta(k,l)$ could be calculated as:

$$\zeta(k,l) = 2\sin\left[\pi\frac{\rho(k,l)}{6}\right] \quad (9)$$

The obtained binomial correlations between the observed daily rainfall amount series were finally taken as the desired correlations of random numbers. Then, the SSRN driving the generation of rainfall amount was reproduced by Eqs. (6) & (7) after calculating the variance-covariance matrix Ω from the desired correlation matrix.

Multisite rainfall stochastic downscaling framework. A stochastic downscaling framework was constructed by linking the parameters of the proposed MSRG to the large-scale circulations at the seasonal scale. First, proper predictors were selected from the NCEP reanalysis dataset by minimizing the regionally averaged mean absolute relative error (MARE) for each model parameter and each season (wet and dry) using a cross-validation procedure (see Section 2.3.2 for more details). Then, least-squares regression models were built between each MSRG parameter (P_{01}, P_{11}, Weibull:shape or Weibull:scale) and the selected predictors for each station and each season during the calibration period 1981–2000 (4 parameters × 2 seasons × 20 stations = 160 regression models). Finally, the MSRG parameters in the validation (1961–1980) or future (2021–2050) period could be predicted based on each regression model using corresponding predictors from the NCEP or GCM outputs. Once the model parameters in the multisite WG were predicted, the multisite series of daily rainfall occurrence and amount for each season could be stochastically reproduced using the corresponding Markov model and Weibull distribution conditioned on 2 sets of SSRNs. The first set of SSRNs, which preserves the spatial correlation of multisite rainfall occurrence, is used for determining if a day is wet or dry by comparing its daily value to the corresponding rainfall transition probability for each station in the occurrence model. The second set of SSRNs, which contains the spatial dependency of multisite rainfall amounts, is applied for stochastically sampling the daily rainfall amount from the corresponding Weibull distribution for each station. Finally, the multisite daily rainfalls for either the wet or dry season over the TRB are simultaneously reproduced based on the proposed multisite rainfall stochastic downscaling framework.

2.3.2. Predictor selection

The choice of large-scale predictors is one of the most crucial processes for developing a stochastic downscaling model because it largely determines the characteristics of the downscaled scenarios (Wilby & Wigley 2000). The basic requirements for predictor selection are that the chosen predictors must not only contribute to the rainfall variability in the current climate and likely change under enhanced greenhouse gas conditions (Schoof et al. 2010), but also could reflect the impacts among different regions and seasons (Timbal et al. 2008). Based on previous studies (Wetterhall et al. 2006, Timbal et al. 2008, Schoof et al. 2010, W. B. Liu et al. 2013b), 16 widely used predictors were considered in this study, including specific humidity, air temperature, zonal and meridional wind speed and sea level pressure at the surface and various pressure levels (500, 700 and 850 hPa). Two conservative approaches for preparing candidate predictors, which consider the impacts of both spatial domain and seasons, were adopted. (1) The first approach (Schoof et al. 2010) takes averaged large-scale predictors over the grid boxes in which the stations are located, and 2 more grid boxes in each cardinal direction (resulting in 25 grids × 2.5° × 2.5° regional average for each predictor; referred to as 'predictors calculated from process 1'). (2) The second approach for predictor calculation (W. B. Liu et al. 2013b) obtained 4 group results (north-south, west-east, northwest-southeast and northeast-southwest gradients; differences between 2 corresponding adjacent grids); we thus called them process 2, process 3, process 4 and process 5, corresponding to process 1 for the first approach. Consequently, 160

(16 basic predictors × 5 processes × 2 seasons) candidate predictors were obtained through the application of the 2 approaches.

The next step is to choose the regionally consistent predictors by minimizing the regionally averaged MARE (%) for each model parameter in each season using a cross-validation procedure (Schoof et al. 2010). The optimal predictors were chosen (Table 2), and the corresponding MARE values for different parameters and seasons over the TRB are shown in Fig. 4. Overall, rainfall was predicted with relatively low skill in the dry season compared to the wet season. The possible reason is that rainfall in the TRB has obvious seasonal characteristics: more rainfall in summer and autumn (>80%) and less rainfall (mainly snowfall) in autumn and winter (<20%). The relatively larger MARE values during the dry season are associated with small absolute errors, since fewer rainfall events occur during this season, resulting in smaller values for model parameters (P_{01}, P_{11}, Weibull:shape or Weibull:scale) (Schoof et al. 2010). However, the MARE values still exhibit smaller magnitude than the interannual variability (simply measured as the coefficient of variation for the seasonal values) for all parameters, which indicates that the skills of the selected predictors are acceptable and could be applied for modeling multisite rainfall characteristics (Schoof et al. 2010).

2.3.3. Empirical downscaling for minimum and maximum temperature

Future daily maximum and minimum temperatures ($T_{adj,fut,d}$), which are the essential input parameters for hydrological models used in this study, were empirically downscaled from the GCM outputs through the constant scaling method (also called the delta change method or perturbation method; Mpelasoka & Chiew 2009, Chen et al. 2013). It adjusts the observed daily maximum and minimum temperatures by adding the difference in these temperatures between the future (2021–2050) and the reference (1971–2000) periods projected by the GCMs:

$$T_{adj,fut,d} = T_{obs,d} + (\bar{T}_{GCM,fut,m} - \bar{T}_{GCM,ref,m}) \quad (10)$$

2.3.4. Hydrological models: SWAT and HIMS

SWAT is a physically based distributed hydrological model for predicting the impacts of climate and land management practices on hydrology in complex watersheds with heterogeneous soil and land use conditions. It divides a basin into a series of subbasins and organizes input information into the following categories: hydrologic response units, groundwater, climate, ponds-wetlands and the main reach draining each basin. During the past 2 decades, this model has been successfully used in different countries and basins (Arnold et al. 1998, Edmonds & Norman 2005, Bekele & Knapp 2010, Zhang et al. 2012, W. B. Liu et al. 2013a). More details for the model can be found in Neitsch et al. (2005), Edmonds & Norman (2005) and Bekele & Knapp (2010).

HIMS is a modular-based multiscale hydrological modeling system consisting of a hydrological information system and a hydrological model library which has integrated several distributed, semi-distributed and lumped hydrological models (Wang et al. 2005, Liu et al. 2008). It divides the catchment into several grid cells with different soil, vegetation

Table 2. Selected predictor variables for rainfall generator parameters in the wet (April to September) and dry (October to March) seasons. P_{01} and P_{11} are the conditional probabilities for the first-order Markov chain; Weibull:shape and Weibull:scale describe the shape and scale parameters of the Weibull distribution, respectively. slp: sea level pressure; shum: specific humidity; airtemp: air temperature; uwnd and vwnd: zonal and meridional components, respectively, of the wind at the surface level. Numbers after variables: corresponding pressure levels; **bold**: different change gradients adopted for certain variables

Season	P_{01}	P_{11}	Weibull:shape	Weibull:scale
Wet	slp	slp(**E-W**)	slp(**NE-SW**)	slp(**N-S**)
	shum700(**E-W**)	shum850(**E-W**)	shum700(**E-W**)	shum500(**NE-SW**)
	airtemp(**NE-SW**)	airtemp700(**E-W**)	airtemp850(**NW-SE**)	airtemp700(**E-W**)
	uwnd850(**NW-S**E)	uwnd850(**NE-SW**)	uwnd	uwnd500(**E-W**)
	vwnd(**NW-S**E)	vwnd(**NW-SE**)	vwnd700(**E-W**)	vwnd(**N-S**)
Dry	slp	slp(**N-S**)	slp(**NW-SE**)	slp
	shum850(**E-W**)	shum500	shum700(**E-W**)	shum700(**NW-SE**)
	airtemp700	airtemp700	airtemp700(**NE-SW**)	airtemp850(**E-W**)
	uwnd700(**NW-SE**)	uwnd850	uwnd(**E-W**)	uwnd(**N-S**)
	vwnd500(**NE-SW**)	vwnd(**E-W**)	vwnd850(**N-S**)	vwnd850(**N-S**)

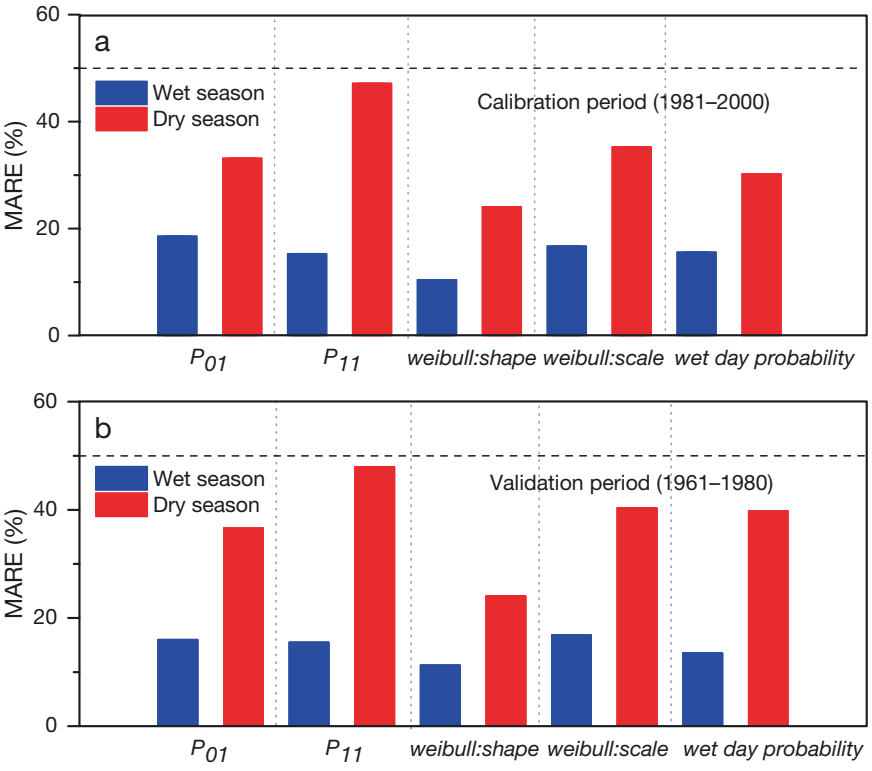

Fig. 4. Mean absolute relative errors (MAREs) of the simulated parameters (2 transition probabilities and 2 parameters of the Weibull distribution) estimated from the selected predictors, with the parameters calculated from rainfall observation during (a) the calibration (1981–2000) and (b) validation (1961–1980) periods

and land use properties and considers many hydrological processes at the grid and basin scale such as precipitation, evaporation, snowmelt, interception, infiltration, subsurface runoff, channel routing and reservoir regulation (Wang et al. 2005). Moreover, it can easily be compatible with an optimization algorithm and can obviously lessen the computation consumption in the model calibration period (Jiang et al. 2013). During the past few years, HIMS has been successfully applied for flood forecasting, water resources planning and climate impact studies in the Yellow River, Haihe River and Heihe River of China and 331 catchments in Australia (L. F. Liu et al. 2013). For more information about the model development and model structure, please refer to Wang et al. (2005) and Jiang et al. (2013).

3. RESULTS AND DISCUSSION

3.1. MSRG performance

The proposed MSRG was first calibrated on a half-year basis (wet and dry seasons) during the period 1981–2000 because of the availability of high-quality rainfall data and was then validated during the period 1961–1980. The corresponding results, which compared the annual rainfall, wet days, 90th quantiles of daily rainfall and mean consecutive wet and dry days simulated by the MSRG against the observed rainfall characteristics, are shown in Figs. 5 & 6. Overall, it reproduced reasonable daily characteristics for the wet season, with the percentile correlations (pct Rs) all >0.94, the Pearson correlations (prs Rs) all >0.72 and the mean relative errors (MREs) all <5.0% for wet season rainfall, rain days, the 90th percentile of daily rainfall and mean consecutive wet and dry days during the calibration and validation periods (Fig. 5). During the dry season, the MSRG results for daily characteristics were also acceptable, with the pct Rs and prs Rs all >0.95 and >0.72, respectively, and the MREs all <6.0% (Fig. 6). The MSRG performance was then validated for the whole year (Fig. 7); results showed that the pct Rs and prs Rs were all >0.93 and >0.76, respectively, and the MREs were all <3.0%. Additionally, the performance of the proposed MSRG for simulating interannual variability, which is critical for hydrological modeling, was also assessed. Results indicated that the MSRG could basically capture the reasonable annual variability for the wet season, dry season and the whole year (Fig. 8). Although MSRG performance was overall slightly worse in the validation period than in the calibration period, probably because of the limitations of linearly linking the model parameters to large-scale predictors, the obtained results are basically accept-

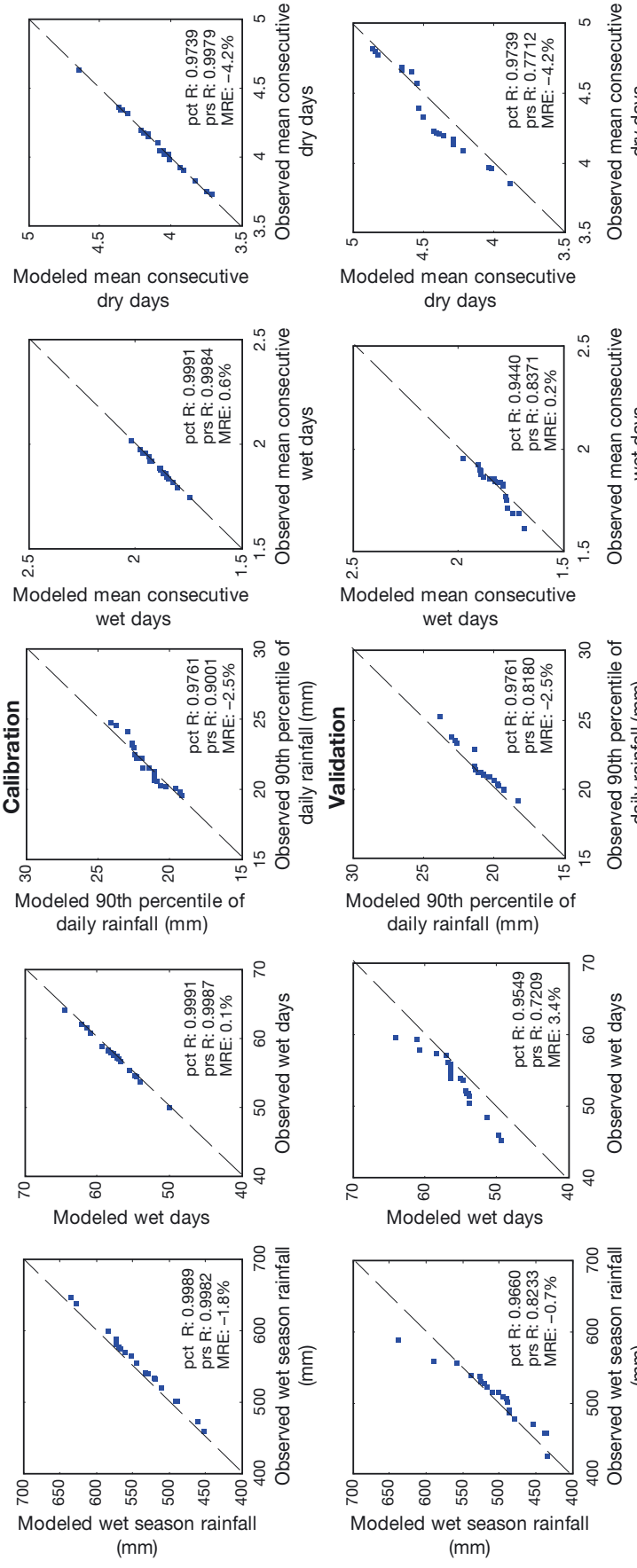

Fig. 5. Performance of the proposed rainfall generator in modeling annual and daily rainfall statistics for the wet season (top: calibration; bottom: validation). pct R: percentile correlation; prs R: Pearson correlation; MRE: mean relative error

able for hydrological implications in this basin.

The performance of the proposed MSRG for modeling the multisite rainfall spatial correlations during the calibration and validation periods is shown in Fig. 9. In this figure, the Pearson correlations of rainfall occurrence and amount series between each station pair against its distance are drawn for both the observed and simulated daily rainfall products. The figure indicates that the MSRG could reasonably catch the correlations of both daily rainfall occurrences and amounts for station pairs from near to far by comparing them to the corresponding results of observations. Although the simulated spatial correlations were slightly overestimated for the relatively far station pairs during the validation period, the spatial correlations of both the multisite rainfall occurrence and amount series were overall acceptable, with the Pearson correlations of scatter points between simulations and observations 0.98 and 0.98, respectively, for the occurrence model and 0.95 and 0.98, respectively for the amount model during the calibration and validation periods (Fig. 9). Additionally, the simulated spatial dependencies for the occurrence model are slightly better in the calibration period than in the validation period, while the simulated spatial dependencies for the amount model are the inverse. The results obtained further certified that the modified SSRN method proposed by Mhanna & Bauwens (2012) was applicable for extending the SSRG to a multisite approach in the stochastic framework. Moreover, the treatment for the process when calculating the needed correlation matrix for the SSRN has obviously been simplified in both occurrence and amount models, which provided the modified SSRN method with the potential to be used for relatively larger basins or regions.

3.2. Calibration and validation for hydrological models

The hydrological models (SWAT and HIMS) were first calibrated for the whole basin based on the model inputs (for example, maximum and minimum temperature, rain-

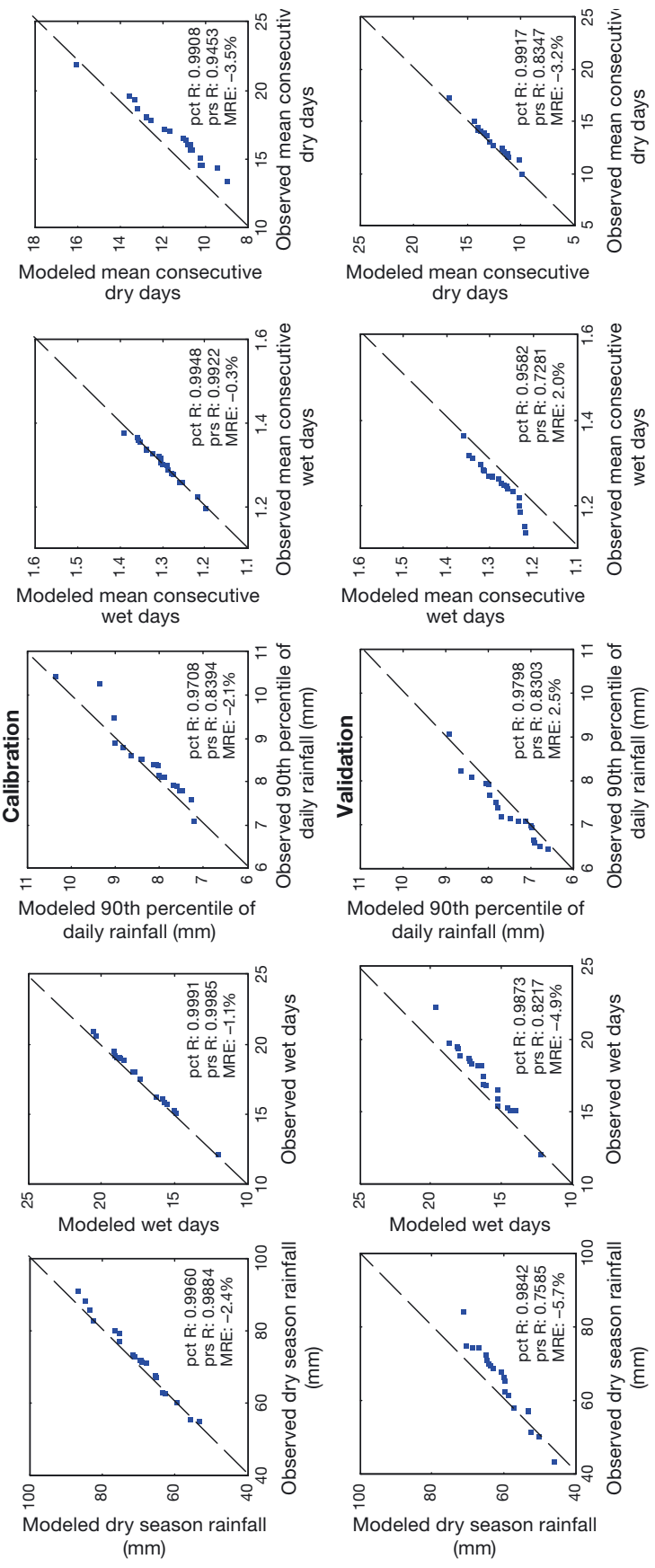

Fig. 6. Performance of the proposed rainfall generator in modeling annual and daily rainfall statistics for the dry season (top: calibration; bottom: validation). Abbreviations as in Fig. 5

fall, digital elevation model, land use map and soil map) and observed daily streamflow (Chenming station) during the period 1981–2000 and then validated during the period 1965–1980 (Figs. 10 & 11). The SWAT model was calibrated using the shuffled complex evolution method (Neitsch et al. 2005), while the HIMS model was calibrated using the random optimization algorithm (Wang et al. 2005). Results showed that they could both simulate reasonable annual and monthly streamflow in the TRB. Specifically, the relative error (RE), correlation coefficient (Cor) and Nash-Sutcliffe coefficient of efficiency values (NSE) between observed and SWAT-simulated annual streamflow were –2.40%, 0.97 and 0.92, respectively, during the calibration period and –0.40%, 0.97 and 0.92, respectively, during the validation period (Fig. 10). For the monthly simulation, they were –3.80%, 0.94 and 0.87, respectively, for the calibration period and –2.2%, 0.92 and 0.83, respectively, for the validation period, which indicated that the overall performance of the SWAT model in the TRB is basically acceptable based on the criteria proposed by Moriasi et al. (2007). The HIMS model performed relatively better than the SWAT model, with RE, Cor and NSE values between observed and simulated annual streamflow of 0.20%, 1.00 and 0.99, respectively, for the calibration period and 0.01%, 0.99 and 0.99, respectively, for the validation period (Fig. 11). Monthly results were 0.70%, 0.95 and 0.95, respectively, for the calibration period and 0.20%, 0.94 and 0.94, respectively, for the validation period. Overall, both hydrological models showed good applicability for historical streamflow simulation and were adequate for future streamflow prediction in the TRB.

3.3. Influences of future climate change on streamflow in the TRB

Generally, annual temperature over the TRB downscaled from multiple GCMs (Fig. 12) would consistently increase by 0.49 to 2.95°C (multiple model average, MMA: 1.71°C) for scenario RCP4.5 and by 1.12 to 3.13°C (MMA: 1.99°C) for scenario RCP8.5 in the future (2021–2050) relative to the reference observed period (1971–2000). However, there are no obvious changes found for future annual rain-

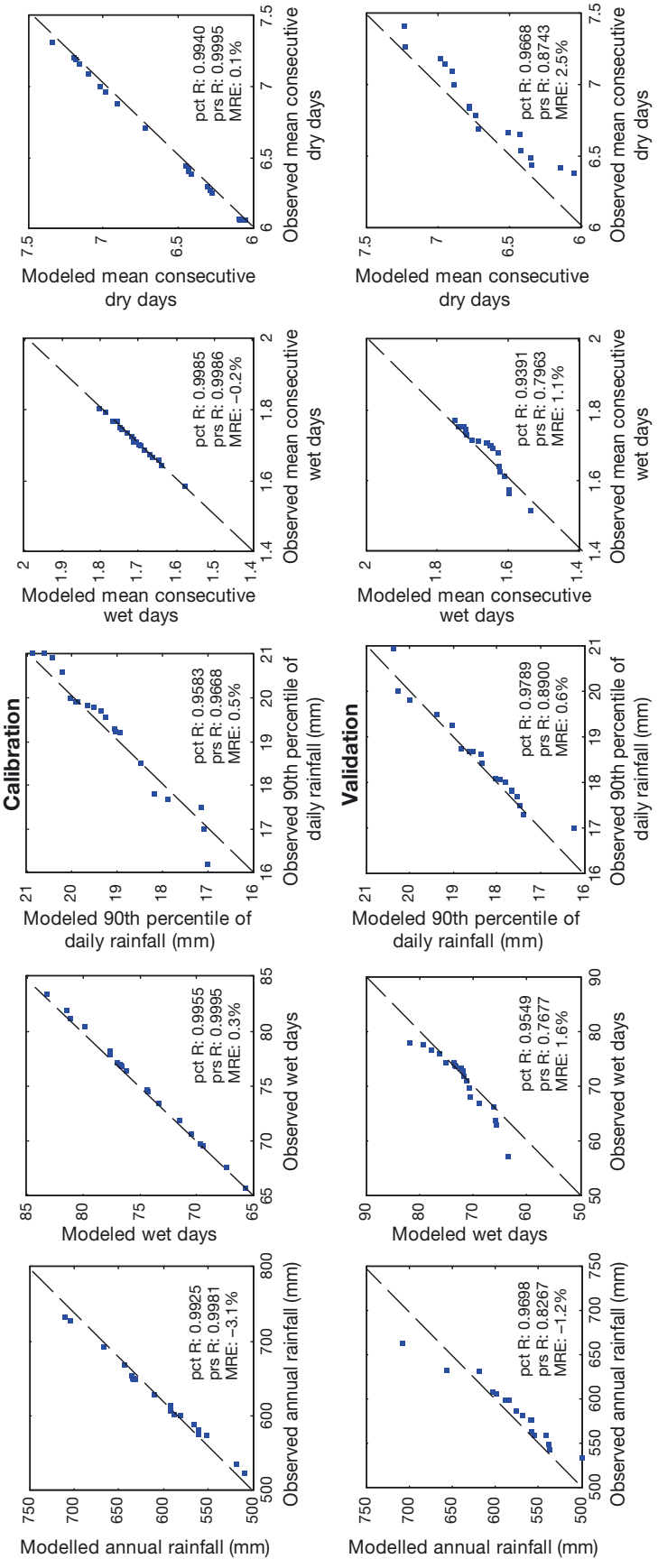

Fig. 7. Performance of the proposed rainfall generator in modeling annual and daily rainfall statistics for the whole year (top: calibration; bottom: validation). Abbreviations as in Fig. 5

fall, with the change ranging from −3.87 to 10.90% (MMA: 1.04%) for scenario RCP4.5 and from −3.84 to 9.87% (MMA: −0.38%) for scenario RCP8.5. The signs of the changes projected for annual rainfall and temperature are in agreement with the historical climate over the TRB (W. B. Liu et al. 2013a) as well as other regional results in northeastern China (Liu et al. 2005, 2011, Zhai et al. 2005, Piao et al. 2010) during the past half-century. Also, they are consistent with GCM results from the IPCC Fourth Assessment (Feng et al. 2011), Fifth Assessment (Xu & Xu 2012) and regional climate model (RCM) results (S. Y. Liu et al. 2013). Correspondingly, compared to the reference period (1971–2000), the annual streamflow in the outlet gauge would decline by −22.02 to 9.29% (MMA: −7.43%) for the SWAT model and by −18.85 to approx. −5.79% (MMA: −11.08%) for the HIMS model for the RCP4.5 scenario and even more for the RCP8.5 scenario (−23.37 to 1.23% [MMA: −11.91%] for the SWAT model and −20.02 to approx. −4.23% [MMA: −12.70%] for the HIMS model). The projected median changes for annual streamflow are basically consistent, although the predicted uncertainties are relatively larger for the SWAT model compared to the HIMS model. Also, the projected sign of future annual streamflow change in Chenming station is consistent with that from the period 1964–2006 (W. B. Liu et al. 2013a). The decreased annual streamflow, which is probably attributed to the annual evapotranspiration increase induced by enhanced annual temperature, would lead to a water availability decline over the entire basin in the near future (2021–2050).

The impacts of future climate change (2021–2050) on streamflow were also conducted for the half-year period (wet and dry seasons) over the TRB (Fig. 13). Similar to the annual results, the temperature in the wet season would increase by 0.46 to 2.50°C (MMA: 1.54°C) for scenario RCP4.5 and by 0.85 to 2.98°C (MMA: 1.8°C) for scenarios RCP8.5; rainfall would remain almost unchanged for both scenarios, with changes of −5.47 to 9.69% (MMA: 0.53%) and −5.85 to 9.49% (MMA: −0.42%) in the wet season relative to the reference period (1971–2000). However, the wet season streamflow at the Chenming gauge were projected to consis-

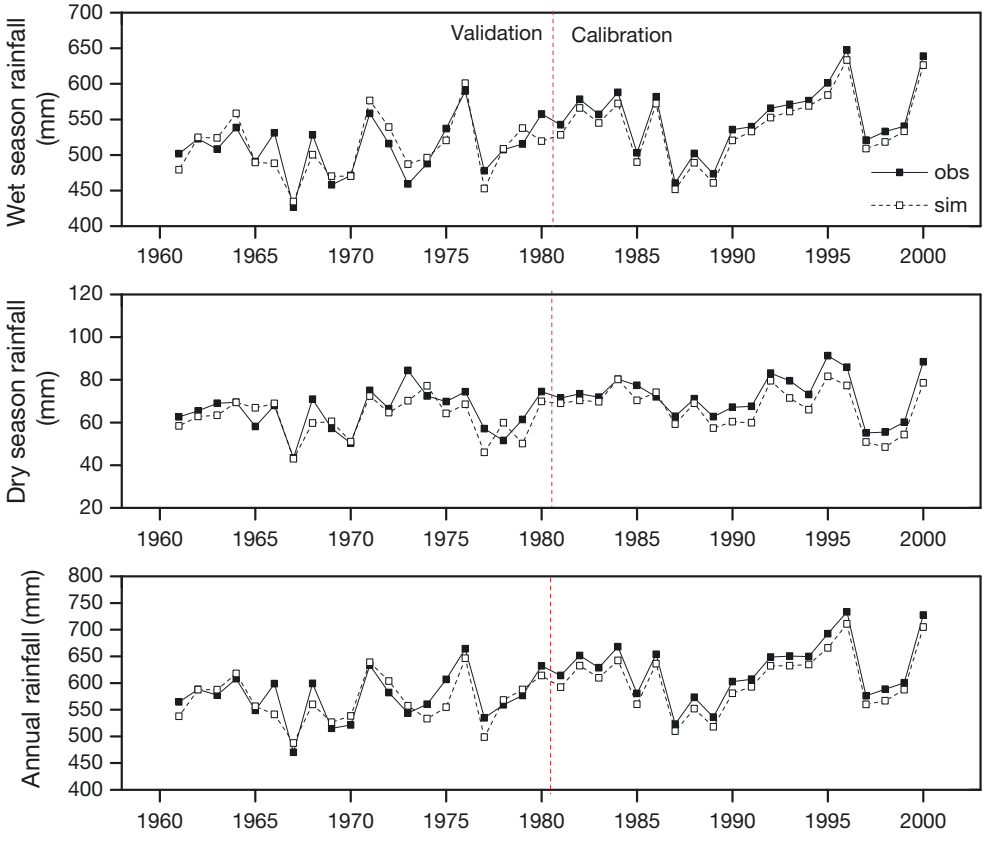

Fig. 8. Performance of the proposed rainfall generator in simulating interannual variability for annual, wet season and dry season rainfall

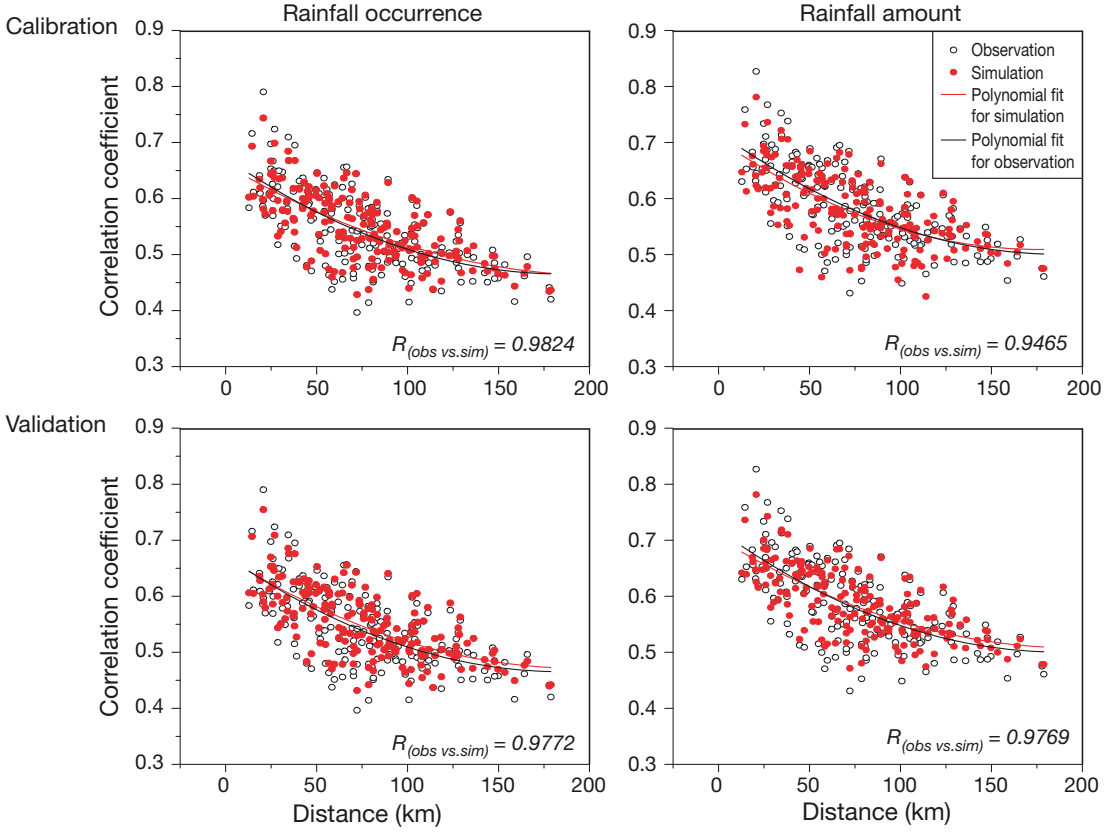

Fig. 9. Performance of the proposed rainfall generator in simulating spatial dependencies in the daily rainfall occurrence and amount model during the validation (1961–1980) and calibration (1981–2000) periods. Distance (*x*-axis): distance between any 2 meteorological stations; dots: Pearson correlations between each station pair

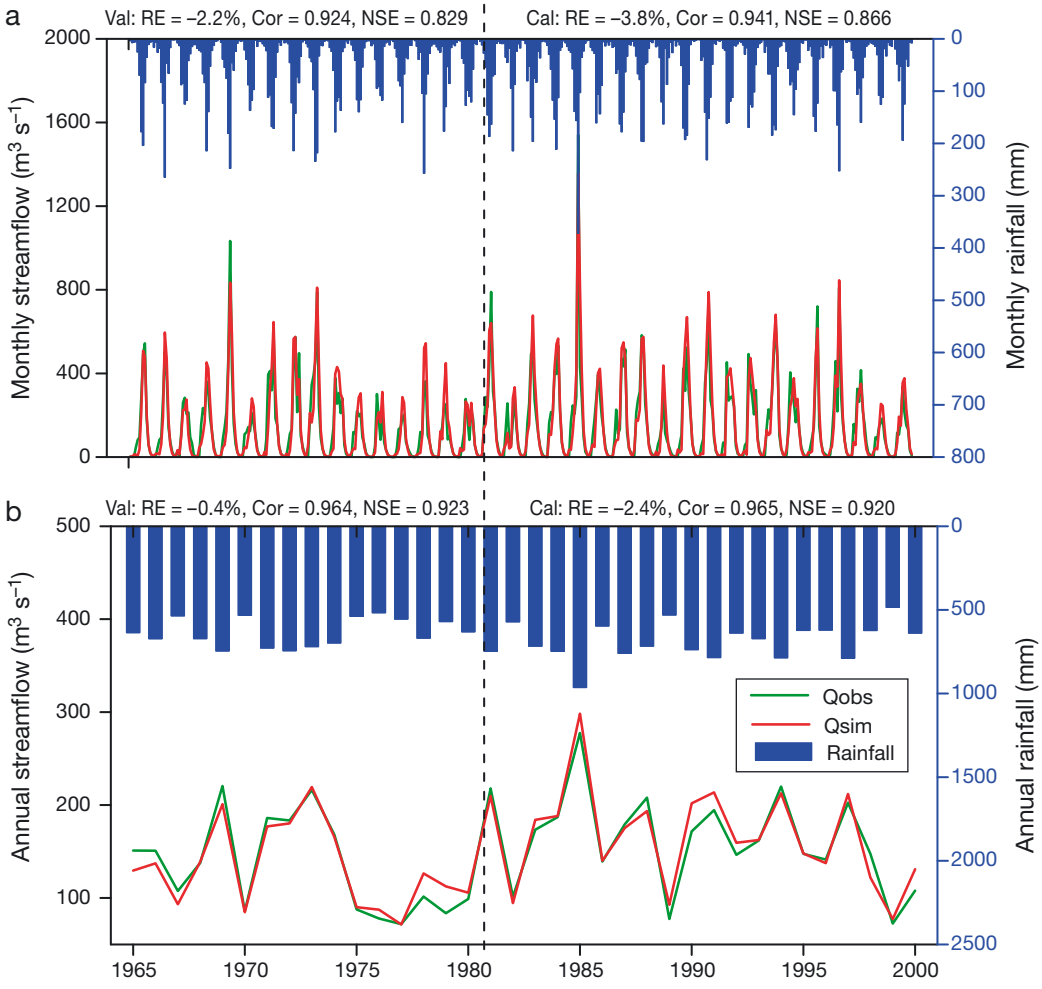

Fig. 10. Soil and Water Assessment Tool simulated and observed (a) monthly and (b) annual streamflow in Chenming gauges during the validation (Val) (1965–1980) and calibration (Cal) (1981–2000) periods. RE: relative error; Cor: correlation coefficient; NSE: Nash-Sutcliffe coefficient of efficiency values; Q: streamflow; sim: simulated; obs: observed

tently decrease among multiple GCMs, with change rates from −0.18 to approx. −28.45% (RCP4.5, MMA: −12.01%) and −0.17 to −29.36% (RCP8.5, MMA: −13.78%) for the SWAT model and from −7.24 to approx. −17.44% (RCP4.5, MMA: −12.49%) and −5.72 to −17.39% (RCP8.5, MMA: −17.90%) for the HIMS model. The projected changes of hydrometeorological variables in the wet season are basically consistent with their historical changes (1960–2006) for summer and autumn in the TRB (W. B. Liu et al. 2013a). Moreover, the temperature and rainfall changes in the wet season are also in agreement with winter and spring results from the Model for Interdisciplinary Research on Climate (MIROC)-driven RegCM3 (S. Y. Liu et al. 2013). The results showed that the decreased wet season streamflow during the period 2021–2050 is closely related to the increased seasonal temperature, which causes more total evapotranspiration over this basin.

Compared to the wet season, the dry season temperature over the TRB (Fig. 14) would increase more, with changes ranging from 0.53 to 3.39°C (MMA: 1.90°C) for scenario RCP4.5 and from 1.08 to 3.78°C (MMA: 2.18°C) for scenarios RCP8.5 during the future period (2021–2050). Moreover, dry season rainfall would slightly increase (changes ranging from −21.16 to approx. 21.96% [MMA: 4.43%]) for scenario RCP4.5 and would slightly decrease (changes ranging from −28.03 to approx. 27.06% [MMA: 2.39%]) for scenario RCP8.5. The streamflow in the dry season projected through multi-GCMs would show an overall increase, with changes ranging from −4.00 to approx. 45.63% (SWAT, MMA: 10.90%) and −2.39 to approx. 7.55% (HIMS, MMA: 2.40%) for scenario RCP4.5 and from −1.53 to approx. 48.86% (SWAT, MMA: 11.83%) and −0.61 to approx. 7.60% (HIMS, MMA: 4.29%) for scenario RCP8.5. Also, the median changes for

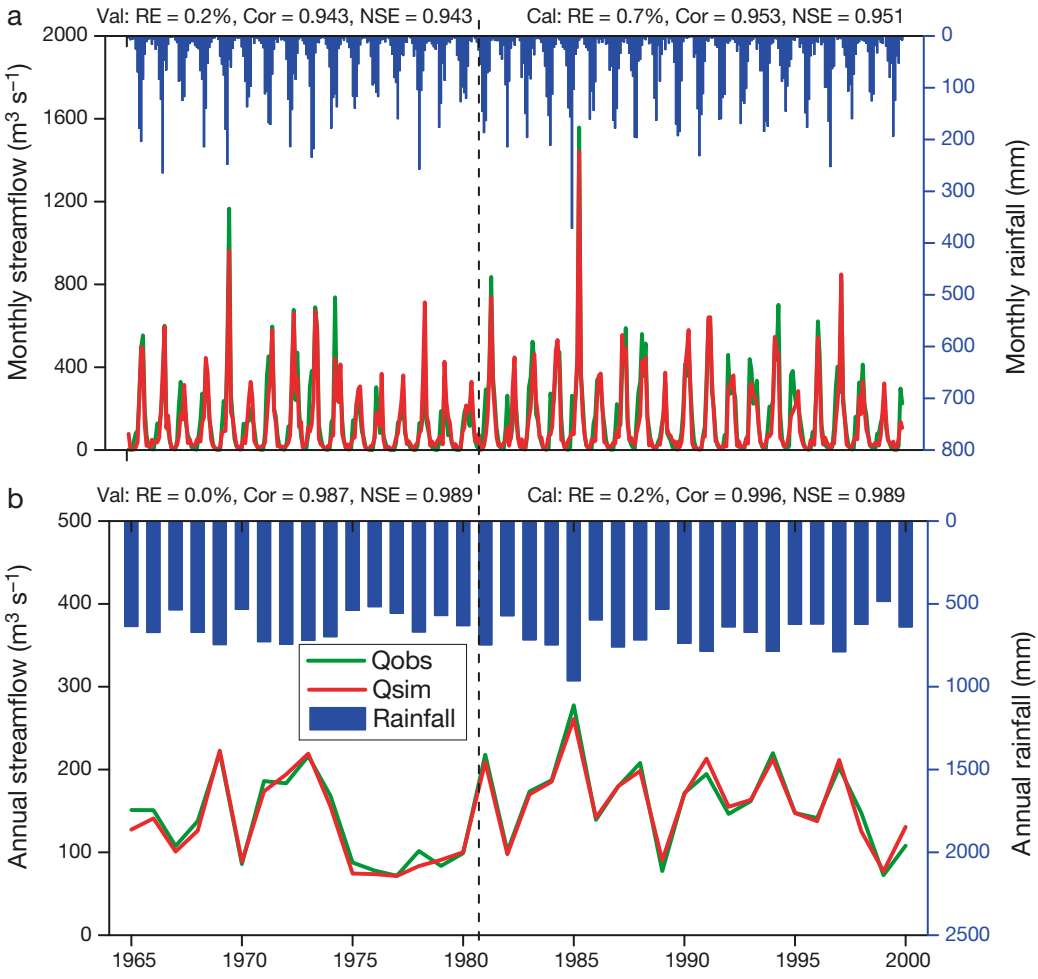

Fig. 11. Hydro-Informatic Modeling System simulated and observed (a) monthly and (b) annual streamflow in Chenming gauges during the validation (Val) (1965–1980) and calibration (Cal) (1981–2000) periods. RE: relative error; Cor: correlation coefficient; NSE: Nash-Sutcliffe coefficient of efficiency values; Q: streamflow; sim: simulated; obs: observed

dry season streamflow projected by both hydrological models are consistent. The increased rainfall and snowfall, combined with rising temperature, would result in more snowmelt runoff, and thus would increase the dry season total streamflow. The temperature and rainfall changes in the dry season during the period 2021–2050 are coincident with their historical (1960–2006) changes in spring and especially winter over the TRB (L. F. Liu et al. 2013) or all of northeastern China (Liu et al. 2005, 2011, Zhai et al. 2005, Piao et al. 2010) and are also in agreement with seasonal results obtained from the RCM (S. Y. Liu et al. 2013). The increased dry season streamflow during the period 2021–2050 would provide more water for forest and agricultural ecosystems and would be helpful for reducing the influences of 'spring drought' during March to April in this basin.

3.4. Uncertainties

The results presented in this study are unavoidably associated with several uncertainties. The primary uncertainties may arise from the output of the GCMs, which is related to their numerical schemes, parameterization, resolution, natural variability and uncertainty in anthropogenic climate forcing factors (Maraun et al. 2010). Although multiple GCMs were used in this study, there remain certain uncertainties inherited from original GCMs which cannot be avoided in the statistical downscaling process at the current stage. For example, the projected changes of annual and dry season streamflow showed a wide range of uncertainties, which may arise from the uncertainties in the multi-GCM rainfall and temperature projections (Figs. 12 & 14).

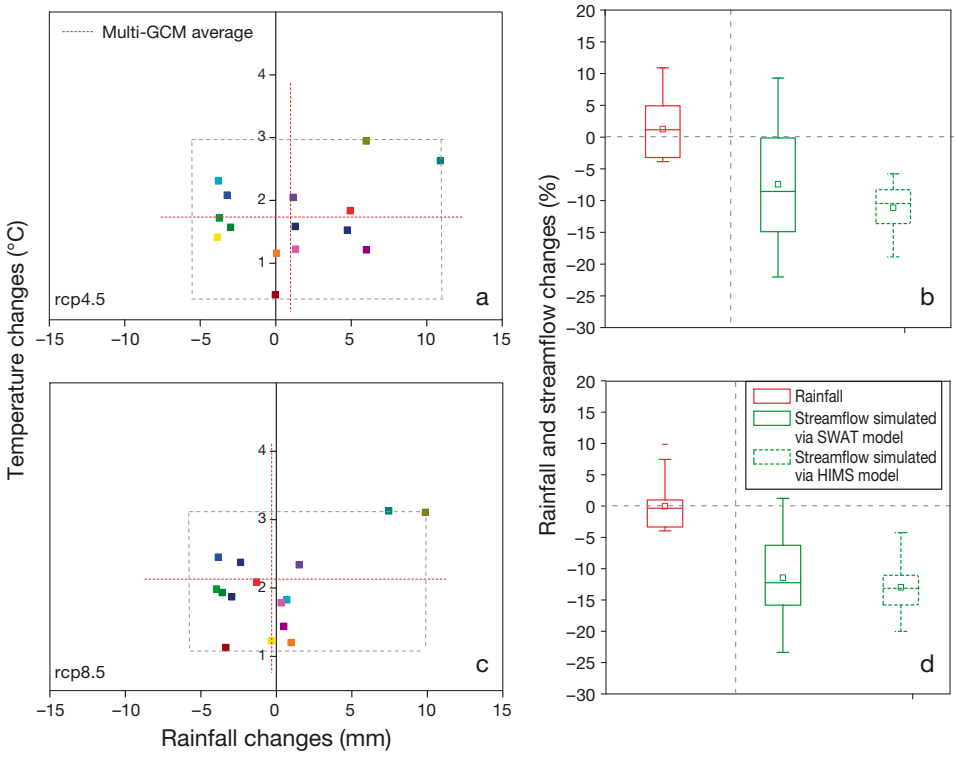

Fig. 12. Projected changes for (a,c) annual temperature, and (b,d) rainfall and streamflow, during the period 2021–2050 (relative to the reference period 1971–2000) for 2 emissions scenarios: (a,b) representative concentration pathway (rcp) 4.5 and (c,d) rcp8.5. Dots with different colors in the left panels: different climate scenarios projected via 15 global climate models (GCMs). Boxplots in the right panels (representing projected rainfall and streamflow among all GCMs) — dashes: outliers; whiskers minimum and maximum values; boxes: 1st and 3rd quartiles; central line: median; small square: mean; SWAT: Soil and Water Assessment Tool; HIMS: Hydro-informatic Modelling System. The vertical dashed line separates rainfall and streamflow results

The second source of uncertainties is associated with the statistical downscaling models, which assume that the relationship between predictor and daily rainfall will remain the same in the future. It is a critical caveat for all statistical downscaling. If the relationship between the MSRG parameters and large-scale predictors is non-stationary in future climate change scenarios, then statistical downscaling techniques may be inappropriate. This is a challenging issue and difficult to test. Additionally, GCMs do not perfectly reproduce predictor variables used by stochastic downscaling, therefore requiring bias correction. This bias correction may not hold into the future, leading to some uncertainties in the result. In addition, the different greenhouse gas emission scenarios, unchanged assumption of future solar radiation, wind speed and humidity changes in the hydrological models, and different parameterization schemes of hydrological models applied could also bring more uncertainties. Despite these caveats, the overall consistency among the downscaled GCM results provide us with some confidence in the streamflow scenarios presented.

4. SUMMARY AND CONCLUSIONS

This paper proposed a simple MSRG by combining the approaches of both Schoof et al. (2010) and Mhanna & Bauwens (2012), which modeled the rainfall occurrence and amount separately with a first-order Markov chain and a 2-parameter Weibull distribution. The most important feature of the proposed MSRG is that it can simulate the spatial dependencies of multisite daily rainfall occurrences and amounts simultaneously using the SSRN method. It has been certified with high efficiency and can to some extent overcome the problem of 'non-positive definiteness of the covariance matrix' when calculating the needed correlation matrices to generate the multisite random numbers (Mhanna & Bauwens 2012). The proposed MSRG was proved not only to have the ability to reproduce reasonable daily rainfall statistics, but also to have the potential to be implemented in relatively large basins or regions. Additionally, a stochastic downscaling framework was constructed based on the MSRG by linking the model parameters to large-scale predictors at the seasonal scale. The impacts of

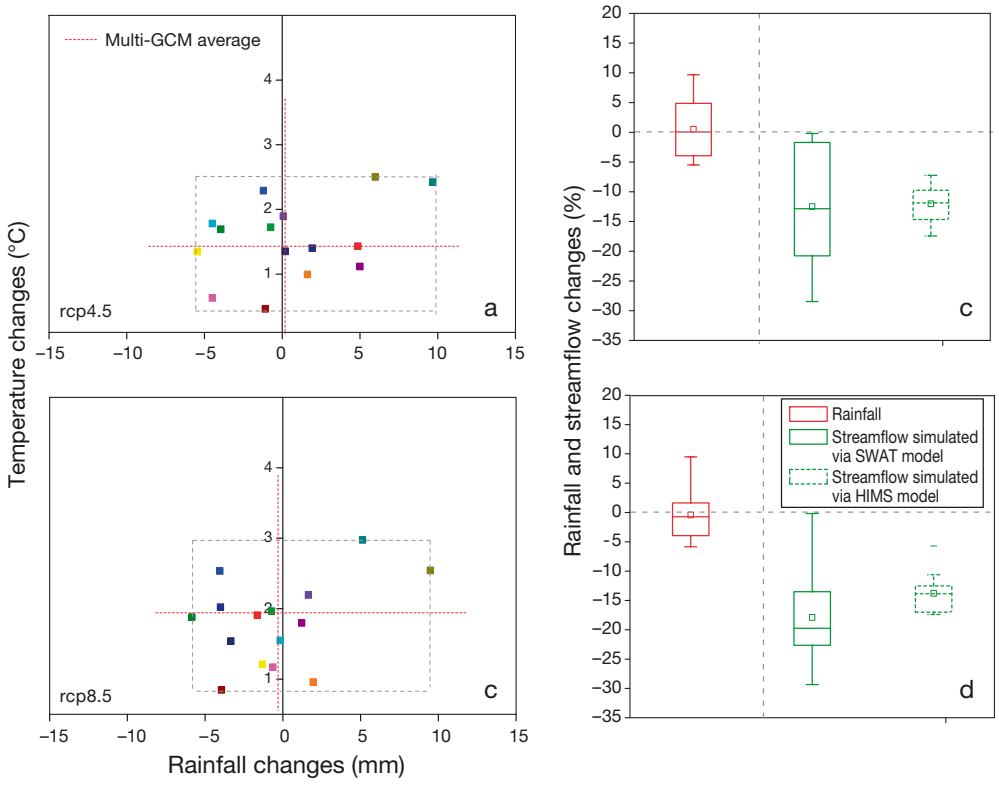

Fig. 13. Projected changes for annual temperature, rainfall and streamflow during the wet season, 2021–2050. See Fig. 12 for further details

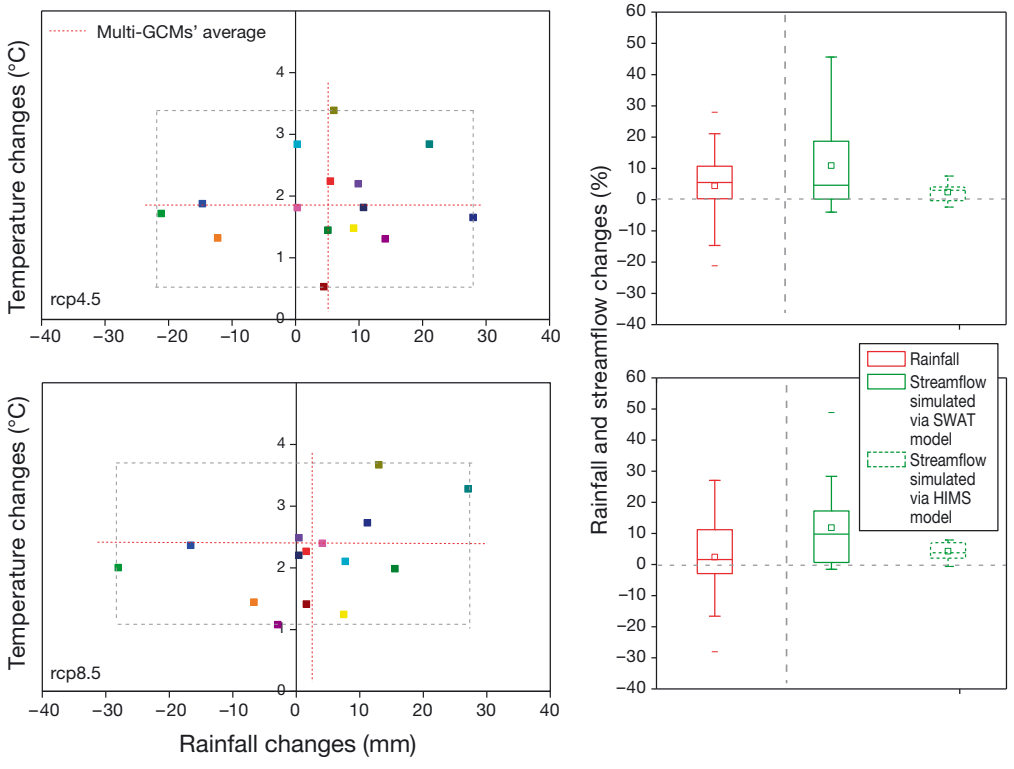

Fig. 14. Projected changes for annual temperature, rainfall and streamflow during the dry season, 2021–2050. See Fig. 12 for further details

future climate on streamflow in the TRB were finally projected using 2 hydrological models (SWAT and HIMS), which are driven by future (2021–2050) local rainfall and temperature scenarios downscaled from GCM simulations of CMIP5 under 2 emission scenarios (RCP4.5 and RCP8.5). The annual and wet season streamflow would overall decrease, while the dry season streamflow would slightly increase over the entire TRB in the future (2021–2050) relative to the reference (1971–2000) period. Consequently, water resources and the corresponding flood risk over the TRB would decline in the wet season and the whole year, while the 'spring drought' during March to April would to some extent be ameliorated because of the slightly increased water availability in the dry season in the near future (2021–2050). Although the projected future annual and wet season rainfall are almost unchanged, the increased total evapotranspiration resulting from the increased temperature is the primary reason for streamflow decline (especially for scenario RCP8.5). In addition, the increased streamflow in the dry season could be attributed to the increase in snowmelt runoff resulting from the increases in both snowfall and temperature in winter. The projected results in this paper could provide a glimpse into a very plausible future for the water resources management community in this mountain basin.

Acknowledgements. This study was financially supported by the Key Technologies Research and Development Program of China (2013BAB05B03), the National Natural Science Foundation of China (Grants 41322001 and 41401037) and the Postdoctoral Science Foundation of China (2014M550850). L.W. is supported by the Hundred Talents Program of the Chinese Academy of Sciences; G.F. is supported by the Australia-China Research Centre on River Basin Management. We thank the editor and all 4 anonymous reviewers for their invaluable comments and constructive suggestions used to improve the quality of the manuscript.

LITERATURE CITED

Arnold JG, Srinisvan R, Muttiah RS, Williams JR (1998) Large area hydrologic modeling and assessment. I. Model development. J Am Water Resour Assoc 34:73–89

Bates B, Kundzewicz ZW, Wu S, Palutikof J (eds) (2008) Climate change and water. Technical paper of the Intergovernmental Panel on Climate Change, IPCC Secretariat, Geneva. Available at www.ipcc.ch/pdf/technical-papers/climate-change-water-en.pdf (accessed 4 March 2014)

Bekele EG, Knapp HV (2010) Watershed modeling to assessing impacts of potential climate change on water supply availability. Water Resour Manag 24:3299–3320

Benestad RE, Hanssen-Bauer I, Chen DL (2008) Empirical-statistical downscaling. World Scientific Publishing, Singapore

Chandler RE, Wheater HS (2002) Analysis of rainfall variability using generalized linear models: a case study from the west of Ireland. Water Resour Res 38:1192

Charles SP, Bates BC, Smith IN, Hughes JP (2004) Statistical downscaling of daily precipitation from observed and modeled atmospheric fields. Hydrol Processes 18: 1373–1394

Chen H, Xu CY, Guo SL (2012) Comparison and evaluation of multiple GCMs, statistical downscaling and hydrological models in the study of climate change impacts on runoff. J Hydrol (Amst) 434–435:36–45

Chen J, Brissette FP, Chaumont D, Braun M (2013) Performance and uncertainty evaluation of empirical downscaling methods in quantifying the climate change impacts on hydrology over two North American river basins. J Hydrol (Amst) 479:200–214

Dawadi S, Ahmad S (2012) Changing climatic conditions in the Colorado River basin: implications for water resources management. J Hydrol (Amst) 430–431:127–141

Edmonds JA, Norman JR (2005) Climate change impacts for the conterminous USA: an integrated assessment summary. Clim Change 69:151–162

Fan L, Fu C, Chen D (2005) Review on creating future climate change scenarios by statistical downscaling techniques. Adv Earth Sci 20:320–329 (in Chinese with English Abstract)

Feng L, Zhou TJ, Wu B, Li T, Luo JJ (2011) Projection of future precipitation change over China with a high-resolution global atmospheric model. Adv Atmos Sci 28: 464–476

Fowler HJ, Blenkinsop S, Tebaldi C (2007) Linking climate change modeling to impacts studies: recent advances in downscaling techniques for hydrological modeling. Int J Climatol 27:1547–1548

Frost AJ, Charles SP, Timbal B, Chiew FHS and others (2011) A comparison of multi-site daily rainfall downscaling techniques under Australian conditions. J Hydrol (Amst) 408:1–8

Fu GB, Charles SP, Chiew FHS, Teng J and others (2013) Modelling runoff with statistically downscaled daily site, gridded and catchment rainfall series. J Hydrol (Amst) 492:254–265

Guo SL, Wang JX, Xiong LH, Ying AW, Li DF (2002) A macro-scale and semi-distributed monthly water balance model to predict climate change impacts in China. J Hydrol (Amst) 268:1–15

Hanssen-Bauer I, Achberger C, Benestad RE, Chen D, Førland EJ (2005) Statistical downscaling of climate scenarios over Scandinavia. Clim Res 29:255–268

Harrison M, Waylen P (2000) A note concerning the proper choice for Markov model order for daily precipitation in the humid tropics: a case study in Costa Rica. Int J Climatol 20:1861–1872

Hewitson BC, Crane RG (2006) Consensus between GCM climate change projections with empirical downscaling: precipitation downscaling over South Africa. Int J Climatol 26:1315–1337

Immerzeel WW, van Beek LPH, Bierkens MFP (2010) Climate change will affect the Asian water towers. Science 328:1382–1385

Jiang Y, Li XY, Huang CC (2013) Automatic calibration a hydrological model using a master–slave swarms shuffling evolution algorithm based on self-adaptive particle swarm optimization. Expert Syst Appl 40: 752–757

Kalnay E, Kanamitsu M, Kirtler R, Collins W and others (1996) The NCEP/NCAR 40-year reanalysis project. Bull Am Meteorol Soc 77:437–471

Kienzle SW, Nemeth MW, Byrne JM, MacDonald RJ (2012) Simulating the hydrological impacts of climate change in the upper North Saskatchewan River basin, Alberta, Canada. J Hydrol (Amst) 412–413:76–89

Lennartsson J, Baxevani A, Chen D (2008) Modelling precipitation in Sweden using multiple step Markov chains and a composite model. J Hydrol (Amst) 363:42–59

Li C, Singh VP, Mishra AK (2012) Simulation of the entire range of daily precipitation using a hybrid probability distribution. Water Resour Res 48:W03521, doi:10.1029/2011WR011446

Liao Y, Liu L, Chen D, Xie Y (2011) An evaluation of the BCC/RCG-WG's performance in simulating daily non-precipitation variables in China. Acta Meteorol Sin 69: 310–319 (in Chinese with English Abstract)

Liu BH, Xu M, Henderson M, Qi Y (2005) Observed trends of precipitation amount, frequency, and intensity in China, 1960–2000. J Geophys Res 110:D08103

Liu CM, Wang ZG, Zheng HX, Zhang L, Wu XF (2008) Development of hydro-informatic modelling system and its application. Sci China Ser E 51:456–466

Liu LF, Liu CM, Wang ZG, Jiang Y, Zhang YQ, Sang YF, Wang H (2013) Parameter uncertainty of HIMS model and its influence factor analysis. Prog Geogr 32:532–537 (in Chinese with English Abstract)

Liu SY, Gao W, Liang XZ (2013) A regional climate model downscaling projection of China future climate change. Clim Dyn 41:1871–1884

Liu WB, Cai TJ, Ju CY, Fu GB, Yao YF, Cui XQ (2011) Assessing vegetation dynamics and their relationships with climatic variability in Heilongjiang province, northeast China. Environ Earth Sci 64:2013–2024

Liu WB, Cai TJ, Fu GB, Zhang AJ, Liu CM, Yu HZ (2013a) The streamflow trend in Tangwang River basin in northeast China and its difference response to climate and land use change in sub-basins. Environ Earth Sci 69: 51–62

Liu WB, Fu GB, Liu CM, Charles SP (2013b) A comparison of three multisite statistical downscaling models for daily rainfall in the North China Plain. Theor Appl Climatol 111:585–600

Liu WB, Fu GB, Liu CM, Song XY, Ouyang RL (2013c) Projection of future for the North China Plain using two statistical downscaling models and its hydrological implications. Stoch Environ Res Risk Assess 27:1783–1797

Maraun D, Wetterhall F, Ireson AM, Chandler RE and others (2010) Precipitation downscaling under climate change: recent developments to bridge the gap between dynamical models and the end user. Rev Geophys 48:RG3003, doi:10.1029/2009RG000314

Mehrotra R, Sharma A (2007) Preserving low-frequency variability in generated daily rainfall sequences. J Hydrol (Amst) 345:102–120

Mehrotra R, Srikanthan R, Sharma A (2006) A comparison of three stochastic multi-site precipitation occurrence generators. J Hydrol (Amst) 331:280–292

Mhanna M, Bauwens W (2012) A stochastic space-time model for the generation of daily rainfall in the Gaza Strip. Int J Climatol 32:1098–1112

Moriasi DN, Arnold JG, van Liew MW, Bingner RL, Harmel RD, Veith TL (2007) Model evaluation guidelines for systematic quantification of accuracy in water simulations. Trans ASABE 50:885–900

Mpelasoka FS, Chiew FHS (2009) Influence of rainfall scenario construction methods on runoff projection. J Hydrometeorol 10:1168–1183

Neitsch SL, Arnold JG, Kiniry JR, Srinivasan RS, Williams JR (2005) Soil and water assessment tool: theoretical documentation, version 2005. Available at http://swatmodel.tamu.edu/media/1292/ swat2005theory.pdf (accessed 4 March 2014)

Piao S, Ciais P, Huang Y, Shen Z and others (2010) The impacts of climate change on water resources and agriculture in China. Nature 467:43–51

Qian B, Corte-Real J, Xu H (2002) Multisite stochastic weather model for impact studies. Int J Climatol 22: 1377–1397

Richardson CW (1981) Stochastic simulation of daily precipitation, temperature, and solar radiation. Water Resour Res 17:182–190

Sachindra DA, Huang F, Barton AF, Perera BJC (2014) Multi-model ensemble approach for statistical downscaling general circulation model outputs to precipitation. QJR Meteorol Soc 140:1161–1178

Schoof JT, Pryor SC, Surprenant J (2010) Development of daily precipitation projections for the United States based on probabilistic downscaling. J Geophys Res 115: D13106, doi:10.1029/2009JD013030

Srikanthan R, Pegram GGS (2006) Stochastic generation of multi-site rainfall occurrences. Adv Geosci 6:1–10

Srikanthan R, Pegram CGS (2009) A nested multisite daily rainfall stochastic generation model. J Hydrol (Amst) 371:142–153

Taylor KE, Stouffer RJ, Meehl GA (2012) An overview of CMIP5 and the experiment design. Bull Am Meteorol Soc 93:485–498

Thompson CS, Thomson PJ, Zheng XG (2007) Fitting a multisite daily rainfall model to New Zealand data. J Hydrol (Amst) 340:25–39

Timbal B, Fernandez E, Li Z (2008) Generalization of a statistical downscaling model to provide local climate change projections for Australia. Environ Model Softw 24:342–358

Wan H, Zhang X, Barrow EM (2005) Stochastic modeling of daily precipitation of Canada. Atmos-Ocean 43:23–32

Wang ZG, Zheng HX, Liu CM (2005) A modular framework of distributed hydrological modeling system: hydro-informatic modeling system, HIMS. Prog Geogr 24: 109–115 (in Chinese with English Abstract)

Wang W, Shao Q, Yang T, Peng S, Xing W, Sun F, Luo Y (2013) Quantitative assessment of the impact of climate variability and human activities on runoff changes: a case study in four catchments of the Haihe River basin, China. Hydrol Process 27:1158–1174

Wetterhall F, Bárdossy A, Chen DL, Halldin S, Xu CY (2006) Daily precipitation-downscaling techniques in three Chinese regions. Water Resour Res 42:W11423, doi:10.1029/2005WR004573

Wilby RL, Wigley TML (2000) Precipitation predictors for downscaling: observed and general circulation model relationships. Int J Climatol 20:641–661

Wilby RL, Dawson CW, Barrow EM (2002) SDSM-a decision support tool for the assessment of regional climate change impacts. Environ Model Softw 17:145–157

Wilks DS (1989) Rainfall intensity, the Weibull distribution, and estimation of daily surface runoff. J Appl Meteorol 28:52–58

Wilks DS (1998) Multisite generalization of a daily stochastic precipitation generation model. J Hydrol (Amst) 210: 178–191

Wilks DS (1999) Interannual variability and extreme-value characteristics of several stochastic daily precipitation models. Agric For Meteorol 93:153–169

Xu CH, Xu Y (2012) The projection of temperature and precipitation over China under RCP scenarios using a CMIP multi-model ensemble. Atmos Ocean Sci Lett 5:527–533

Yang C, Chandler RE, Isham VS, Wheater HS (2005) Spatial-temporal rainfall simulation using generalized linear models. Water Resour Res 41:W11415, doi:10.1029/2004WR003739

Zhai PM, Zhang XB, Wan H (2005) Trends in total precipitation and frequency of daily precipitation extremes over China. J Clim 18:1096–1108

Zhang AJ, Zhang C, Fu GB, Wang BD, Bao ZX, Zheng HX (2012) Assessments of impacts of climate change and human activities on runoff with SWAT for the Huifa River basin, northeast China. Water Resour Manage 26: 2199–2217

Zheng XG, Katz RW (2008) Simulation of spatial dependence in daily rainfall using multisite generators. Water Resour Res 44:W09403, doi:10.1029/2007WR006399

Editorial responsibility: Toshichika Iizumi, Tsukuba, Japan

Submitted: March 4, 2014; Accepted: August 6, 2014
Proofs received from author(s): November 25, 2014